Amino acid oxidation of the D1 and D2 proteins by oxygen radicals during photoinhibition of Photosystem II

Ravindra Kale[a], Annette E. Hebert[b], Laurie K. Frankel[b], Larry Sallans[c], Terry M. Bricker[b,1], and Pavel Pospíšil[a,1]

[a]Department of Biophysics, Centre of the Region Haná for Biotechnological and Agricultural Research, Faculty of Science, Palacký University, 783 71 Olomouc, Czech Republic; [b]Department of Biological Sciences, Division of Biochemistry and Molecular Biology, Louisiana State University, Baton Rouge, LA 70803; and [c]The Rieveschl Laboratories for Mass Spectrometry, Department of Chemistry, University of Cincinnati, Cincinnati, OH 45221

Edited by Robert Haselkorn, University of Chicago, Chicago, IL, and approved February 3, 2017 (received for review November 16, 2016)

The Photosystem II reaction center is vulnerable to photoinhibition. The D1 and D2 proteins, lying at the core of the photosystem, are susceptible to oxidative modification by reactive oxygen species that are formed by the photosystem during illumination. Using spin probes and EPR spectroscopy, we have determined that both $O_2^{\bullet-}$ and $HO^{\bullet}$ are involved in the photoinhibitory process. Using tandem mass spectroscopy, we have identified a number of oxidatively modified D1 and D2 residues. Our analysis indicates that these oxidative modifications are associated with formation of $HO^{\bullet}$ at both the Mn_4O_5Ca cluster and the nonheme iron. Additionally, $O_2^{\bullet-}$ appears to be formed by the reduction of O_2 at either $Pheo_{D1}$ or Q_A. Early oxidation of D1:^{332}H, which is coordinated with the Mn1 of the Mn_4O_5Ca cluster, appears to initiate a cascade of oxidative events that lead to the oxidative modification of numerous residues in the C termini of the D1 and D2 proteins on the donor side of the photosystem. Oxidation of D2:^{244}Y, which is a bicarbonate ligand for the nonheme iron, induces the propagation of oxidative reactions in residues of the D-*de* loop of the D2 protein on the electron acceptor side of the photosystem. Finally, D1:^{130}E and D2:^{246}M are oxidatively modified by $O_2^{\bullet-}$ formed by the reduction of O_2 either by $Pheo_{D1}^{\bullet-}$ or $Q_A^{\bullet-}$. The identification of specific amino acid residues oxidized by reactive oxygen species provides insights into the mechanism of damage to the D1 and D2 proteins under light stress.

photosynthesis | Photosystem II | reactive oxygen species | photo inhibition | mass spectrometry

Photosystem II (PSII) functions as a water-plastoquinone oxidoreductase (1, 2) and is a thylakoid membrane pigment–protein complex present in all oxygenic photosynthetic organisms (cyanobacteria, algae, and higher plants). Current high-resolution structures of thermophilic cyanobacterial PSII (3, 4), and lower resolution structures of the red algal (5) and higher plant photosystems (6), have been critically important in furthering our understanding of the molecular organization of PSII. Structurally, the PSII reaction center core is composed of five proteins: D1, D2, the α- and β-subunits of cytochrome b_{559}, and PsbI. These components bind all of the redox-active cofactors of PSII.

Excitation energy transfer and electron transport within PSII are unavoidably associated with production of reactive oxygen species (ROS) when the absorption of light by the chlorophyll antenna exceeds the capacity for energy utilization. Many mechanisms for ROS production have been proposed (for reviews, see refs. 7 and 8). Briefly, singlet oxygen ($^1O_2$) may be formed by excitation energy transfer from triplet chlorophylls (formed either by the change in orientation of the spin of an excited electron in the PSII antenna complex, or via charge recombination of the primary radical pair $^3[P_{680}^{\bullet+}Pheo^{\bullet-}]$) to O_2 (9, 10). ROS production by electron transport involves either the two-electron oxidation of water or the one-electron reduction of O_2 on the PSII electron donor and acceptor sides, respectively. On the PSII electron donor side, a two-electron oxidation of water leads to the formation of hydrogen peroxide (H_2O_2), which may be oxidized to the superoxide anion radical ($O_2^{\bullet-}$) or reduced to the hydroxyl radical ($HO^{\bullet}$) (8). It has been proposed that H_2O_2 is oxidized either by the redox-active tyrosine residue $Tyr_Z^{\bullet+}$ (11) or the chlorophyll cation $Chl_Z^{\bullet+}$ (12). H_2O_2 may be reduced to $HO^{\bullet}$ by free manganese released from damaged Mn_4O_5Ca clusters (13). On the PSII electron acceptor side, a one-electron reduction of O_2 forms $O_2^{\bullet-}$, which is known to initiate a cascade of reactions leading to the formation of both H_2O_2 and $HO^{\bullet}$ (7). Redox-active cofactors known to reduce O_2 to $O_2^{\bullet-}$ are pheophytin ($Pheo^{\bullet-}$), the tightly bound plastosemiquinone at the Q_A site ($Q_A^{\bullet-}$), the loosely bound plastosemiquinone at the Q_B site ($Q_B^{\bullet-}$), free plastosemiquinone ($PQ^{\bullet-}$), and the ferrous heme iron in the low potential (LP) form of cyt b_{559} (8). Free H_2O_2 is formed by dismutation of $O_2^{\bullet-}$, known to occur spontaneously or catalyzed by either cyt b_{559} or the superoxide dismutase attached to the stromal side of the thylakoid membrane in the vicinity of PSII. Alternatively, bound peroxide may be formed by the interaction of $O_2^{\bullet-}$ with the nonheme iron (14). In this reaction, a ferric-peroxo species is formed, the protonation of which produces a ferric-hydroperoxo species. The reduction of free H_2O_2 or bound peroxide can form $HO^{\bullet}$ via the Fenton reaction.

Light-induced production of ROS by PSII is accompanied by inevitable damage to the D1 and D2 proteins. This damage consists of initial protein oxidation events, which subsequently leads to cleavage and aggregation of the D1 subunit (15). Protein oxidation, cleavage, and aggregation have also been observed, although to a lesser extent, in the D2 protein, which degrades in a similar manner to the D1 protein but at a slower rate (16). Despite the fact

Significance

Reactive oxygen species (ROS) damage the D1 and D2 reaction center proteins of Photosystem II in a process known as photoinhibition. Photoinhibition is an unavoidable consequence of excitation energy transfer and electron transport. The ROS responsible for oxidative damage, the sites of ROS production, and the residues oxidatively modified have not been determined. In this work, we identify $HO^{\bullet}$ as being produced on both the oxidizing and reducing sides of the photosystem. $O_2^{\bullet-}$ also appears to be produced at either $Pheo_{D1}$ or Q_A. Additionally, residues on the D1 and D2 proteins were identified that are oxidatively modified during a photoinhibitory timecourse. Finally, we propose plausible pathways for the propagation of protein oxidation events in the D1 and D2 proteins.

Author contributions: R.K., T.M.B., and P.P. designed research; R.K., A.E.H., L.S., T.M.B., and P.P. performed research; R.K., T.M.B., and P.P. analyzed data; and L.K.F., T.M.B., and P.P. wrote the paper.

The authors declare no conflict of interest.

This article is a PNAS Direct Submission.

[1]To whom correspondence may be addressed. Email: pavel.pospisil@upol.cz or btbric@lsu.edu.

This article contains supporting information online at www.pnas.org/lookup/suppl/doi:10.1073/pnas.1618922114/-/DCSupplemental.

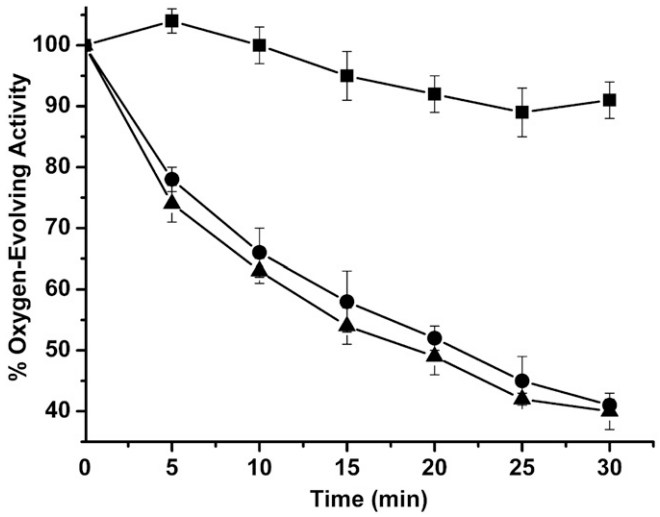

Fig. 1. Timecourse for photoinactivation. PSII membranes (100 μg of Chl·mL^{-1}) were incubated in the dark (squares) or illuminated with high intensity red light either in the absence (circles) or presence (triangles) of 0.4 mM DCBQ + 1 mM FeCN. At various time points, samples were removed and assayed for O_2 evolution capacity. Control O_2 evolution rates were 400–500 μmol O_2·mg^{-1} Chl·h^{-1}. Each point represents the mean value and the SD of three experiments (mean ± SD, $n = 3$).

that D1 and D2 protein damage has been intensively studied over the last three decades, only limited information has been provided concerning the identification of amino acid residues that are oxidized by ROS. On the PSII electron donor side, a number of natively oxidized residues were identified in the vicinity of the Mn_4O_5Ca cluster on the D1, D2, and CP43 subunits (17). On the PSII electron acceptor side, Sharma et al. (18) had identified a peptide of the D1 protein (^{130}E–^{136}R) that lies in the vicinity of $Pheo_{D1}$ and contained a single oxidative modification on an unidentified residue. Subsequently, Frankel et al. (19) identified a number of natively oxidized residues in the vicinity of Q_A and $Pheo_{D1}$. However, a complete study using mass spectrometry to identify D1 and D2 residues oxidatively modified during a photoinhibition timecourse, with the goal of identifying the primary amino acid targets for ROS, has not been performed.

In this work, we provide evidence that the specific oxidation of amino acid residues of the D1 and D2 proteins is associated with the site-specific formation of HO$^•$. We demonstrate that HO$^•$ formed by both at the Mn_4O_5Ca cluster and the nonheme iron is responsible for oxidation of amino acids at the lumenally exposed C terminus of the D1 protein and the stromally exposed D-*de* loop of the D2 protein, respectively. Additionally, $O_2^{•-}$ formed by the reduction of O_2 either by $Pheo_{D1}$ or Q_A oxidizes nearby residues on the D1 and D2 proteins.

Results

Photoinactivation Timecourse Detected by O_2 Evolution. Fig. 1 illustrates the timecourse for photoinactivation monitored by O_2 evolution in red light, both in the absence and presence of electron acceptors. The photoinactivation was similar in both cases, with no significant difference being observed. The loss of O_2 evolution exhibited a half-life of approximately 15–20 min. In the dark, no significant decrease in O_2 evolving capacity was observed. These results are consistent with the hypothesis that the principal site for photoinhibition, under the conditions used in this study, was on the PSII electron donor side. These results are similar to those obtained by Zavafer et al. (20) for red, green, and blue light photoinactivation of the PSII.

Detection of the Superoxide Anion Radical Formation. The light-induced production of $O_2^{•-}$ by PSII membranes was measured by using EPR spin-trapping spectroscopy. The spin trap 5-(ethoxy-carbonyl)-5-methyl-1-pyrroline *N*-oxide (EMPO), which reacts with $O_2^{•-}$ forming the EMPO-OOH adduct, was used. In the dark, no EMPO-OOH adduct EPR signal was observed (Fig. 2*A*, 0 min). Illumination of PSII membranes resulted in the appearance of the EMPO-OOH adduct spectra that exhibit the four peaks and hyperfine splitting characteristics of EMPO-OOH adduct (21). Fig. 2*A* (top trace) shows the characteristic EMPO-OOH adduct EPR signal generated by the control xanthine/xanthine oxidase (X/XOD) system. The time profile of the EMPO-OOH adduct EPR signal indicates that $O_2^{•-}$ is formed relatively rapidly during the illumination timecourse (Fig. 2*B*). Because the EMPO-OOH adduct has a half-life of 8 min, the slight decrease in the EPR signal observed after 8 min of illumination is likely due to the instability of the EMPO-OOH adduct. These observations demonstrate that $O_2^{•-}$ is produced in PSII membranes.

Detection of Hydroxyl Radical Formation. The light-induced production of HO$^•$ in PSII membranes was also measured by using EPR spin-trapping spectroscopy. The α-(4-pyridyl *N*-oxide)-*N*-(tert-butylnitrone) (POBN)/ethanol system was used to detect HO$^•$. The interaction of HO$^•$ with ethanol yields the α-hydroxyethyl radical ($CH(CH_3)HO^•$), which reacts with POBN, forming a stable α-hydroxyethyl radical adduct of POBN (POBN-$CH(CH_3)$OH adduct). In the dark, PSII membranes exhibited no detectable EPR signal (Fig. 2*C*, 0 min). Upon illumination (Fig. 2*C*), the EPR spectrum exhibited the six lines with three equivalent doublets reported for the POBN-$CH(CH_3)$OH adduct spectrum (22).

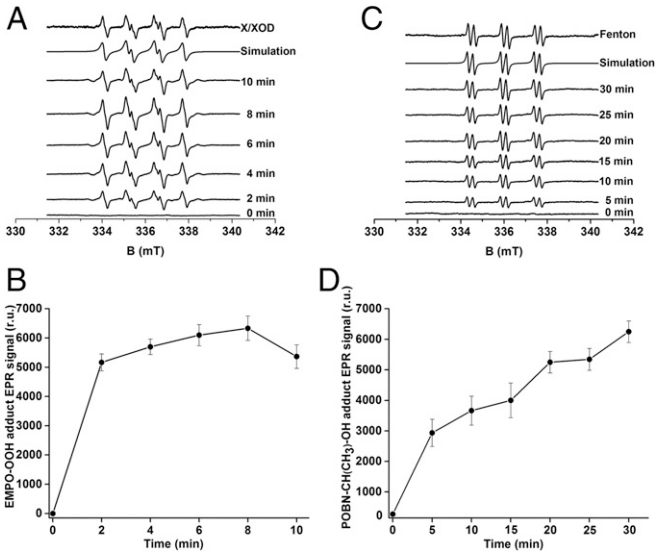

Fig. 2. EPR spectroscopy of light-induced EMPO-OOH and POBN-$CH(CH_3)$OH adducts in PSII membranes. (*A*) EMPO-OOH adduct EPR spectra were obtained after illumination of PSII membranes in the presence of 50 mM EMPO and 40 mM Mes (pH 6.5). Control EMPO-OOH adduct EPR spectrum using the xanthine/xanthine oxidase system and its simulation are shown above. Spectrum obtained at various illumination times are shown below. (*B*) The time profile of the light-induced EMPO-OOH adduct EPR signal. (*C*) POBN-$CH(CH_3)$-OH adduct EPR spectra were obtained after illumination of PSII membranes in the presence of 50 mM POBN, 170 mM ethanol, and 40 mM Mes-NaOH (pH 6.5). Control POBN-OH EPR spectrum obtained using Fenton reagents (200 μM H_2O_2 and 40 μM $FeSO_4$) and its simulation are shown above. Spectrum obtained at various illumination times are shown below. (*D*) The time profile of the light-induced POBN-$CH(CH_3)$OH adduct EPR signal. In *B* and *D*, each point represents the mean value and the SD of at least three experiments with respective units of EPR spectra (mean ± SD, $n = 3$).

Fig. 2*C* (top trace) shows the characteristic POBN-CH(CH_3)OH adduct EPR signal generated by using the Fenton reagent as a control. The time profile of the POBN-CH(CH_3)OH adduct EPR signal shows that $HO^•$ is produced throughout the illumination period (Fig. 2*D*). These results indicate that illumination of PSII membranes results in $HO^•$ production.

Effect of Antioxidants, Chloride, and Nonheme Iron on Hydroxyl Radical Formation. To explore the origin of $HO^•$ formation, the effects of antioxidants, chloride, and nonheme iron on the light-induced POBN-CH(CH_3)OH adduct EPR spectrum were examined. The addition of the enzymatic antioxidants of $O_2^{•-}$ and H_2O_2, superoxide dismutase and catalase, respectively, suppressed the POBN-CH(CH_3)OH adduct EPR signal (Fig. S1*A*). Additionally, when the chelator desferal, a potent inhibitor of the Fenton reaction (23), was used, the POBN-CH(CH_3)OH adduct EPR signal was also decreased. These results indicate that $HO^•$ is formed by reduction of H_2O_2 via Fenton reactions. Fig. S1*B* shows the effects of exogenous chloride, acetate, a chloride-binding inhibitor, and a chloride channel blocker, 4,4′-diisothiocyanatostilbene-2,2′-disulfonic acid (DIDS), on the formation of $HO^•$. The POBN-CH(CH_3)OH adduct EPR signal was reduced significantly in the presence of chloride, acetate, and DIDS. This result indicates that chloride and reagents that modulate chloride binding decreased the POBN-CH(CH_3)OH adduct EPR signal. Fig. S1*C* shows the effect of a nonheme iron ligand, formate, a nonheme iron oxidant, ferricyanide (FeCN), and the exogenous electron acceptor, 2,6-dichlorophenolindophenol (DCPIP), on the formation of $HO^•$. These all decreased the POBN-CH(CH_3)OH adduct EPR signal. These results indicate that both chloride and nonheme iron modulate $HO^•$ formation on the PSII electron donor and acceptor side, respectively.

D1 Protein Oxidation, Cleavage, and Aggregation. Protein radicals ($P^•$) are formed by hydrogen abstraction from amino acid residues and are located either on the protein backbone or residue side chains (24). To determine formation of $P^•$ in PSII membranes, the immuno-spin trapping technique using 5,5-dimethyl-1-pyrroline *N*-oxide (DMPO) was used (25). In this method, the DMPO spin trap interacts with $P^•$, forming a DMPO-P adduct, which is then detected by using immunological techniques with an antibody directed against the nitrone of DMPO (anti-DMPO antibody). When PSII membranes were incubated with DMPO in dark, a 32-kDa band was detected with the anti-DMPO antibody (Fig. 3*A*). After illumination, the intensity of the 32-kDa band increased and an additional 68-kDa band appeared. These results demonstrate that illumination of PSII membranes induced the formation of $P^•$ located on the D1 protein.

Protein carbonyls can be introduced into oxidatively modified proteins by the β-scission of protein alkoxyl radicals, which leads to the formation of carbonyls and protein alkyl radicals (24). To monitor formation of protein carbonyl groups in PSII membranes, immunoblotting using an anti–2,4-dinitrophenylhydrazone (DNP) antibody was performed. In this method, carbonyl groups were first derivatized with 2,4-dinitrophenylhydrazine (DNPH) and the modified proteins were subsequently identified by using an anti-DNP antibody (26). PSII membranes incubated in the dark exhibited a single 32-kDa band. Illumination of the PSII membranes yields the appearance of an additional 68-kDa band (Fig. 3*B*). These results show that illumination of PSII membranes resulted in the formation of protein carbonyl groups located on the D1 protein.

The formation of carbonyls and $P^•$ is associated with protein backbone cleavage (fragmentation) and protein aggregation (protein–protein cross-linking), respectively. To monitor cleavage and aggregation of the D1 protein, immunoblot analysis using antibodies detecting the C terminus of the D1 protein (anti–C-terminal antibody) and the D-*de* loop of the D1 protein (anti–D-*de* loop antibody) was performed. When the anti–C-terminal antibody was used, 32- and 52-kDa bands were observed in dark incubated PSII membranes. Illumination resulted in the appearance of new bands in the 9-, 18-, and 68-kDa molecular mass ranges (Fig. 3*C*) and an increase in the intensity of the 52-kDa band. The anti–D-*de* loop antibody detected a 32-kDa band in the dark, whereas the 9-, 18-, and 68-kDa bands appeared after exposure of PSII membranes to light (Fig. 3*D*). Our data demonstrate that, under our experimental conditions, the 18-kDa peptide arises from the C terminus of the D1 protein and includes the portions of the D-*de* loop bearing the antigenic determinants for the D-*de* loop antibody. A number of other laboratories, using a variety of experimental protocols, have observed a D1 fragment of similar apparent molecular mass (27–29). The higher molecular mass bands at 52 and 68 kDa are aggregates containing D1 and possibly other protein components. These results indicate that illumination of PSII membranes yields cleavage and aggregation of the D1 protein.

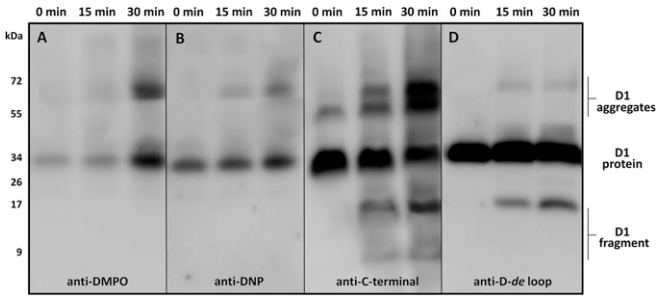

Fig. 3. Immunoblot identifying formation of protein radical, carbonyl group, fragment, and aggregates on the D1 protein. Immunoblot of dark-adapted and high intensity light illuminated PSII membranes labeled with DMPO and identified with an anti-DMPO antibody (*A*), labeled with DNP and identified with an anti-DNP antibody (*B*), identified with an anti–C-terminal antibody (*C*) and identified with an anti–D-*de* loop antibody (*D*). PSII membranes were exposed to high intensity red light for 15 and 30 min, separated by SDS/PAGE and blotted on nitrocellulose membrane and probed with an antibody. Representative blots from three independent experiments are presented. The duration of the high intensity illumination is shown above.

Effect of Antioxidants, Chloride, and Nonheme Iron on Protein Radical and Carbonyl Group Formation in the D1 protein. To explore the origin of $P^•$ and carbonyl group formation, the effects of antioxidants, chloride, reagents that modulate chloride binding with PSII, and reagents that interact with the nonheme iron were examined. The effects of these reagents on the formation of the DMPO-P adduct and DNP-carbonyl derivative were examined by immuoblotting (Fig. S2). The addition of the antioxidants superoxide dismutase, catalase, or mannitol (Fig. S2*A*) lowered the intensity of the 32- and 68-kDa bands labeled with both anti-DMPO and anti-DNP. Additionally, when samples were treated with desferal, a potent inhibitor of the Fenton reaction (23), the intensity of the 68-kDa band labeled with anti-DMPO and anti-DNP was nearly abolished (Fig. S2*A*). These results indicate that suppression of $HO^•$ production decreased the formation of both $P^•$ and protein carbonyl groups on the D1 protein. Fig. S2*B* shows the effects of chloride, acetate (a chloride-binding inhibitor), and DIDS (a chloride channel blocker), on the bands labeled with anti-DMPO and anti-DNP. The addition of chloride and acetate to PSII membranes during illumination lowered the labeling of the 32- and 68-kDa band with both anti-DMPO and anti-DNP. Incubation with DIDS during illumination completely abolished labeling of the 68-kDa band with both anti-DMPO and anti-DNP. These results demonstrate that chloride, and reagents that modulate chloride binding, influence the production of $P^•$ and carbonyl groups on the D1 protein. Fig. S2*C* shows the effects of formate (a nonheme iron ligand), ferricyanide (a nonheme iron oxidant), and DCPIP (an exogenous electron acceptor) on labeling with anti-DMPO and

anti-DNP. All three reagents lowered the intensity of labeling of the 32- and 68-kDa bands with anti-DMPO and anti-DNP. These results indicate that the nonheme iron influences in the formation of $P^{\bullet}$ and carbonyl groups on the D1 protein.

Identification of Oxidized Amino Acid Residues on D1 and D2 Proteins During a Photoinhibitory Timecourse. To identify the oxidative modifications occurring within the D1 and D2 proteins during photoinhibition, samples were examined after 0, 15, and 30 min of illumination. These time-points corresponded to approximately 0, 45, and 60% inhibition of O_2 evolution. The quality of the tandem mass spectra used in this study is illustrated in Fig. S3. The results from these experiments are shown in Table S1 and Fig. 4. Initially, at 0 min, a number of residues were observed to be oxidatively modified, including the D1 residues ^{316}T, ^{317}W, ^{319}D, ^{328}M, ^{331}M, and ^{333}E and the D2 residues ^{18}M, ^{246}M, ^{247}V, and ^{329}M. Most of these residues (D1 residues ^{316}T, ^{317}W, ^{319}D, ^{328}M, ^{331}M, and ^{333}E and the D2 residue ^{329}M) are located in the C-terminal domains of the D1 and D2 subunits and are in close proximity to the Mn_4O_5Ca cluster.

Comparison with this background of natively oxidized residues allows the identification of modifications that are directly the result of experimental photoinhibitory conditions. After 15 min of illumination, a number of additional residues were modified, including the D1 residue ^{332}H and the D2 residues ^{328}W, ^{333}D, ^{334}Q, and ^{336}H. Most of the oxidatively modified residues that were identified at 0 min were also observed after 15 min of illumination. All of the additional residues observed to be modified after 15 min of photoinhibitory illumination are between 2.1 Å (D1:^{332}H) and 32 Å (D2:^{336}H) from the Mn_4O_5Ca cluster and located on the luminal side of PSII. These results indicate that under conditions where 45% of the O_2 evolution capacity of PSII has been lost, modifications of residues in the vicinity of the metal cluster were the first to be observed.

After 30 min of illumination, numerous additional residues on both the D1 and D2 proteins were observed to be oxidatively modified (Table S1). The D1 residues ^{1}M, ^{7}R, ^{130}E, and ^{131}W are located on the stromal side of the protein. D1:^{130}E and D1:^{131}W are particularly interesting and are in close proximity to $Pheo_{D1}$. The D1 residues ^{315}N and ^{329}E are located on the luminal side of the protein in the vicinity of the metal cluster. The additional D2 residues modified at 30 min include ^{242}E, ^{244}Y, and ^{245}S, which are located on the stromal side of the protein in the D-*de*–loop region and are in the vicinity of both the nonheme iron and Q_A. The D2 residues ^{341}F, ^{342}P, ^{343}E, ^{344}E, and ^{345}V are located on the luminal side of the thylakoid membrane in the vicinity of the Mn_4O_5Ca cluster.

Discussion

During the light reactions of photosynthesis, water oxidation and plastoquinone reduction are associated with the accumulation of oxidizing and reducing equivalents on the PSII electron donor and acceptor sides, respectively. These redox equivalents have the ability to form ROS by either partial water oxidation or partial reduction of O_2 (8). It has been hypothesized that $HO^{\bullet}$ is involved in D1 protein damage. This hypothesis was based on the observation that damage to the D1 protein could be initiated by the exogenous addition of H_2O_2 and prevented by exogenous $HO^{\bullet}$ scavengers (27, 30). Similar oxidative modifications to the D2 protein occurs, however, with slower reaction kinetics (16). Oxidation of the D1 and D2 proteins by $HO^{\bullet}$ is initiated by hydrogen atom abstraction from an amino acid residue forming $P^{\bullet}$. $P^{\bullet}$ reacts with O_2, generating an oxygen-centered protein peroxyl radical ($POO^{\bullet}$) that may subsequently oxidize other nearby residues as it is reduced to a protein hydroperoxide (POOH). Direct experimental evidence for the light-induced oxidation of specific amino acid residues on the D1 and D2 proteins by ROS is lacking. Early studies using electrospray ionization mass spectrometry revealed extensive oxidation of the D1 and D2 proteins in dark-treated PSII reaction centers (18). The use of tandem mass spectrometry recently allowed a more comprehensive identification of oxidized amino acids in PSII (31). Amino acids localized in the vicinity of the Mn_4O_5Ca cluster, $Pheo_{D1}$, and Q_A were identified as being oxidatively modified in PSII membranes isolated from field-grown spinach (17, 32). The aim of the present study was to investigate the role of $HO^{\bullet}$ in oxidative damage to the D1 and D2 proteins during photoinhibition and to identify the oxidatively modified residues on these subunit proteins by using mass spectrometry. Our findings indicate that amino acid residues in close proximity to the Mn_4O_5Ca cluster were modified during the early stages of photoinhibition, whereas amino acids near $Pheo_{D1}$, Q_A, and the nonheme iron were modified later in the photoinhibitory timecourse.

PSII Electron Donor Side ROS Production by Incomplete Water Oxidation. The addition of exogenous chloride to PSII membranes significantly suppresses the formation of $HO^{\bullet}$ (Fig. S1*B*). This observation is in agreement with previous reports that chloride-depleted PSII membranes produced more $HO^{\bullet}$ compared with control PSII membranes (33, 34). The involvement of chloride in $HO^{\bullet}$ formation is supported by the observation that acetate and DIDS nearly

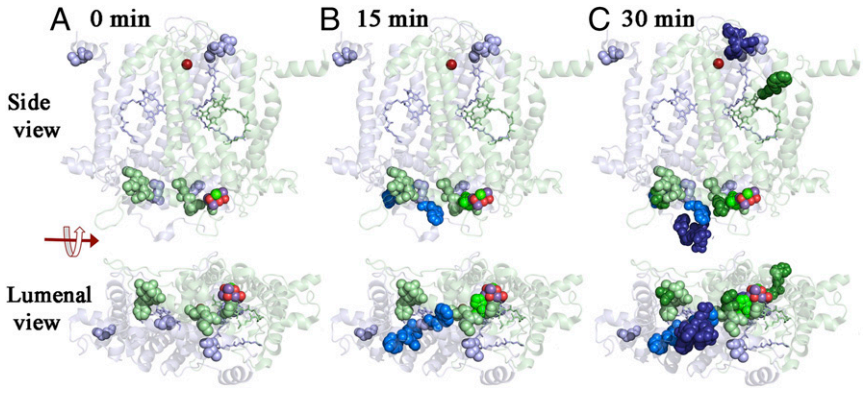

Fig. 4. Oxidative modifications of the D1 and D2 proteins. Time course for the appearance of oxidative modifications of the D1 and D2 proteins presented as side and luminal views. The D1 protein is shown in pale green and the D2 protein is shown in pale blue. Oxidized residues are shown as spheres. Those present at 0 min are shown as pale green (D1) and pale blue (D2). Residues oxidatively labeled at 15 and 30 min are shown in progressively darker shades of green (D1) and blue (D2), respectively. The Mn_4O_5Ca cluster and the nonheme iron are shown as spheres. $Pheo_{D1}$ and Q_A are rendered as pale green and $Pheo_{D2}$ as pale blue sticks, respectively. The protein structure is from spinach PSII (PDB ID code 3JCU; ref. 6) as rendered in PYMOL (51).

abolished detectable $HO^{\bullet}$ production (Fig. S1*B*). It is possible that a water channel plays a crucial role in $HO^{\bullet}$ formation. One hypothesis is that the removal of chloride from a water channel results in the uncontrolled delivery of water to the Mn_4O_5Ca cluster, resulting in the formation of H_2O_2 by incomplete water oxidation. Subsequently, H_2O_2 is reduced to $HO^{\bullet}$ by the Fenton reaction mediated by Mn. Previously, it was demonstrated that removal of chloride during moderate heat treatment of PSII membranes in the dark resulted in the formation of H_2O_2 and, subsequently, $HO^{\bullet}$ production via Fenton reaction (35). One should note that chloride depletion leads to the formation of protein-bound Mn^{2+} (36) possibly facilitating this reaction. Additionally, it is possible that chloride depletion perturbs a proton exit pathway (37). Such disruption could give rise to long-lived higher S states (38, 39) that may increase the probability of the release of partially oxidized water intermediates. These possibilities are not mutually exclusive.

Oxidation of C-Terminal Residues of D1 and D2 Proteins by the Hydroxyl Radical. Oxidized amino acids identified on the PSII electron donor side are located at the C termini of the D1 and D2 proteins and are in close proximity of the Mn_4O_5Ca cluster. D1:^{332}H was identified as being oxidatively modified early in the photoinhibitory timecourse (Fig. 4 and Table S1). This residue is a ligand to Mn1 of the metal cluster (3) and may be associated with a water ingress channel to the oxygen-evolving site (40). We hypothesize that $HO^{\bullet}$ formed by the reduction of H_2O_2 by Mn1, which may partially dissociate from the metal cluster, leads to hydrogen abstraction from D1:^{332}H with subsequent propagation of amino acid oxidation events in the C termini of the D1 and D2 proteins (Fig. S4*A*).

ROS Production by the Reduction of O_2. The one-electron reduction of O_2 on the PSII electron acceptor side leads to $O_2^{\bullet-}$ formation (Fig. 2*A*). Earlier it was shown that interaction of $O_2^{\bullet-}$ with the nonheme iron forms an iron-peroxo intermediate (14). The observation that replacement of bicarbonate by formate suppressed $HO^{\bullet}$ formation supports the hypothesis that nonheme iron is involved in $HO^{\bullet}$ formation. Additionally, when the nonheme iron was oxidized by ferricyanide, $HO^{\bullet}$ formation was essentially eliminated. The artificial electron acceptor DCPIP, which accepts electrons from $Q_A^{\bullet-}$, also significantly suppressed $HO^{\bullet}$ formation (Fig. S1*C*). These data are consistent with the hypothesis that electron transfer from $Q_A^{\bullet-}$ may reduce the bound ferric iron-peroxo intermediate forming $HO^{\bullet}$. $HO^{\bullet}$ generated at the nonheme iron can abstract hydrogen from nearby residues. In the presence of O_2, subsequent propagation of amino acid oxidation reactions may occur in the D-*de* loop of the protein (Fig. S4*B*). It should be noted that $O_2^{\bullet-}$, formed by the reduction of O_2 by $Pheo_{D1}^{\bullet-}$ or $Q_A^{\bullet-}$, may directly modify nearby amino acid residues without first forming the ferric iron-peroxo intermediate (Fig. S4*B*). These mechanisms are not mutually exclusive.

Conclusions

Our results significantly enhance our understanding of the mechanisms of photoinhibition. We have identified specific amino acid residues of the D1 and D2 proteins that are oxidized by $HO^{\bullet}$, and, possibly $O_2^{\bullet-}$, during illumination. Early in the process, $HO^{\bullet}$ is produced by reduction of H_2O_2 formed by incomplete water oxidation, possibly due to uncontrolled water accessibility to the Mn_4O_5Ca cluster or defects in the proton exit pathway. Hydrogen abstraction from D1:^{332}H, coordinated to the Mn_4O_5Ca cluster, by $HO^{\bullet}$ appears to initiate a cascade of amino acid oxidation events at the C termini of the D1 and D2 proteins. Later, formation of $HO^{\bullet}$ at the nonheme iron may be associated with hydrogen abstraction from D2:^{244}Y, with subsequent oxidation events occurring in amino acids of the D-*de* loop of the D2 protein. Finally, $O_2^{\bullet-}$ formed by the reduction of O_2 by $Pheo_{D1}^{\bullet-}$ and/or $Q_A^{\bullet-}$ may oxidatively modify the residues D1:^{130}E and D2:^{246}M.

Materials and Methods

PSII Membrane Isolation. PSII membranes were isolated from fresh spinach leaves (*Spinacia oleracea)* purchased from a local market, by using the method of Berthold et al. (41–43). Before PSII isolation, spinach leaves were kept in darkness to allow for dark adaptation. The PSII membranes were suspended in a buffer solution containing 400 mM sucrose, 10 mM NaCl, 5 mM $CaCl_2$, 5 mM $MgCl_2$, and 50 mM Mes-NaOH (pH 6.5) and stored at −80 °C until use.

Timecourse for Photoinhibition. For these experiments (and the oxidative modification mapping studies described below), the PSII membranes were isolated from spinach leaves incubated overnight at room temperature at a low light intensity (<5 μmol photons·m^{-2}·s^{-1}) to facilitate the partial repair of PSII. After isolation, as described above, the PSII membranes were suspended at 100 μg Chl·mL^{-1} in 400 mM sucrose, 50 mM Mes-NaOH (pH 6.0), 15 mM NaCl, and either incubated in darkness or exposed to red light (663 nm) at 1,400 μmol photons m^{-2}·s^{-1} at room temperature for 0–30 min, either in the presence or absence of 0.4 mM 2,6-dichlorobenzoquinone (DCBQ) + 1 mM potassium ferricyanide. After exposure, the samples were immediately removed from the chamber and assayed for O_2 evolution activity by polarography at room temperature (Hansatech Instruments) using 400 μM DCBQ as an electron acceptor. The control O_2 evolution rate was >400 μmol O_2.mg Chl^{-1}·h^{-1}. For mass spectrometry, samples were removed after 0, 15, and 30 min illumination and stored at −80 °C before electrophoresis. At these time points, the samples exhibited 100, 55, and 40% of control O_2 evolution capability, respectively.

EPR Spin-Trapping Spectroscopy. Free O_2 radicals were detected by EPR spin-trapping spectroscopy. The spin trapping of $O_2^{\bullet-}$ and $HO^{\bullet}$ was accomplished by using the spin traps EMPO (Alexis Biochemicals) or POBN (Enzo), respectively. PSII membranes (150 μg Chl·mL^{-1}) were illuminated in a glass capillary tube (Blaubrand intraMARK) with 25 mM EMPO or 50 mM POBN, 170 mM ethanol, and 40 mM Mes buffer (pH 6.5). The spectra were recorded by using an EPR spectrometer Mini Scope MS400 (Magnettech). The EPR conditions used were as follows: microwave power, 10 mW; modulation amplitude, 1 G; modulation frequency, 100 kHz; sweep width, 100 G; and scan rate, 1.62 G·s^{-1}. For quantification, intensity of the EPR signal was evaluated by the relative height of the peak of the first derivative of the EPR absorption spectrum. In these studies, PSII membranes were illuminated with continuous red light (>600 nm, 1.000 μmol photons m^{-2}·s^{-1}) at room temperature. In some experiments, the following compounds were added individually to the PSII membranes before the onset of illumination: 400 U·mL^{-1} superoxide dismutase, 400 U·mL^{-1} catalase, 5 mM desferal, 100 mM sodium chloride, 100 mM sodium acetate, 10 mM DIDS, 50 mM mannitol, 10 mM sodium formate, 20 μM potassium ferricyanide, and 30 μM DCPIP.

Immunoblot Analysis. For the identification of D1 fragments and aggregates induced by illumination, proteins were resolved by using a Tricine-SDS-polyacrylamide gel electrophoresis (Tricine-SDS/PAGE) (44). Concentrations of acrylamide were 4% (wt/vol) in the stacking and 10/16% (wt/vol) in the resolving gels. PSII membranes (10 μg Chl) were loaded into each well. For Western blot analysis, separated proteins were transferred by using a semidry electroblotter to a nitrocellulose membrane (Bio-Rad Laboratories) and blocked by incubating with 5% (wt/vol) BSA in 25 mM Tris pH 7.6, 150 mM NaCl, 0.05% Tween-20 overnight, and detected by using an antibody against the D-*de* loop of the D1 protein (anti–D-*de* loop antibody) (Agrisera). Goat anti-rabbit IgG (H+L) horseradish peroxidase conjugate (Bio-Rad Laboratories) was used as the secondary antibody. Blots were developed by using the Immobilon Western Chemiluminescent HRP substrate (Merck Spol. s.r.o.) and documented by using a high-resolution digital chemiluminescence imager (Amersham Imager 600, GE Health Care Europe).

Immunoblot Detection of Protein Radicals. Before illumination of the PSII membranes, 50 mM DMPO (Dojindo) was added as a spin trap. After illumination of PSII membranes, electrophoresis, immunoblotting, and blocking the nitrocellulose membrane was probed with a primary rabbit polyclonal antibody against the DMPO nitrone adduct (anti-DMPO antibody) (Abcam) and detected as described above.

Immunoblot Detection of Protein Carbonyl Groups. After illumination of PSII membranes, electrophoresis, and immunoblotting, carbonyl groups in the protein side chains were derivatized to DNP by reaction with 50 mM DNPH for 30 min. After derivatization, the nitrocellulose membrane was blocked as described above and probed with a primary polyclonal rabbit antibody specific to the DNP moiety of the proteins (anti-DNP antibody) (Molecular Probes Europe BV) and detected as described above.

Protein Digestion and Mass Spectrometry. For the identification of oxidatively modified residues, the D1 and D2 proteins were resolved on 12.5–20% acrylamide lithium dodecyl sulfate-PAGE gradient gels by using a nonoxidizing system as was described (17, 45, 46). This nonoxidizing gel system exhibited significantly lower levels of artifactual protein oxidation (see fig. S1 of ref. 17). After electrophoresis, the gels were stained with Coomassie Blue, destained, and the D1 and D2 protein bands were excised. The protein bands were processed for trypsin digestion by using standard protocols. After digestion, the tryptic peptides were processed by using a C18 ZipTip before mass analysis and were resolved by using reversed-phase chromatography. Mass spectrometry was performed on a Thermo Scientific LTQ-FT. For details of the mass spectrometry experimental conditions, see ref. 17.

MassMatrix version 1.3.2 (47, 48) was used for the identification and analysis of peptides containing oxidative mass modifications and was programmed to search for the presence of oxidative modifications on 18 amino acids, excluding glycine and alanine (49, 50). For the identification of oxidative modifications, a P value $\leq 1 \times 10^{-5}$ was required, as was a precursor ion mass precision of $\leq$5.0 ppm. A FASTA library containing the D1, D2, CP47, CP43, PsbO, PsbP, and PsbQ protein sequences and a decoy library containing the same proteins, but with reversed amino acid sequences, were searched. For these experiments, peptides were required to exhibit 0% hits to the decoy library for further consideration.

ACKNOWLEDGMENTS. This work was supported by Ministry of Education, Youth, and Sports of the Czech Republic Grant LO1204 (Sustainable Development of Research in the Centre of the Region Haná from the National Program of Sustainability I) (to R.K. and P.P.), and US Department of Energy, Office of Basic Energy Sciences Grant DE-FG02-09ER20310 (to T.M.B. and L.K.F.). L.S. was supported by the University of Cincinnati.

1. Vinyard DJ, Ananyev GM, Dismukes GC (2013) Photosystem II: The reaction center of oxygenic photosynthesis. *Annu Rev Biochem* 82:577–606.
2. Shen JR (2015) The structure of Photosystem II and the mechanism of water oxidation in photosynthesis. *Annu Rev Plant Biol* 66:23–48.
3. Umena Y, Kawakami K, Shen J-R, Kamiya N (2011) Crystal structure of oxygen-evolving photosystem II at a resolution of 1.9 Å. *Nature* 473(7345):55–60.
4. Suga M, et al. (2015) Native structure of photosystem II at 1.95 Å resolution viewed by femtosecond X-ray pulses. *Nature* 517(7532):99–103.
5. Ago H, et al. (2016) Novel features of eukaryotic Photosystem II revealed by its crystal structure analysis from a red alga. *J Biol Chem* 291(11):5676–5687.
6. Wei X, et al. (2016) Structure of spinach photosystem II-LHCII supercomplex at 3.2 Å resolution. *Nature* 534(7605):69–74.
7. Pospíšil P (2009) Production of reactive oxygen species by photosystem II. *Biochim Biophys Acta* 1787(10):1151–1160.
8. Pospíšil P (2012) Molecular mechanisms of production and scavenging of reactive oxygen species by photosystem II. *Biochim Biophys Acta* 1817(1):218–231.
9. Fischer BB, Hideg É, Krieger-Liszkay A (2013) Production, detection, and signaling of singlet oxygen in photosynthetic organisms. *Antioxid Redox Signal* 18(16):2145–2162.
10. Telfer A (2014) Singlet oxygen production by PSII under light stress: Mechanism, detection and the protective role of β-carotene. *Plant Cell Physiol* 55(7):1216–1223.
11. Chen G-X, Kazimir J, Cheniae GM (1992) Photoinhibition of hydroxylamine-extracted photosystem II membranes: Studies of the mechanism. *Biochemistry* 31(45):11072–11083.
12. Mano J, Takahashi M, Asada K (1987) Oxygen evolution from hydrogen peroxide in photosystem II: Flash induced catalytic activity of water-oxidizing photosystem II membranes. *Biochemistry* 26:2495–2501.
13. Pospíšil P, Šnyrychová I, Nauš J (2007) Dark production of reactive oxygen species in photosystem II membrane particles at elevated temperature: EPR spin-trapping study. *Biochim Biophys Acta* 1767(6):854–859.
14. Pospíšil P, Arató A, Krieger-Liszkay A, Rutherford AW (2004) Hydroxyl radical generation by photosystem II. *Biochemistry* 43(21):6783–6792.
15. Yamamoto Y (2001) Quality control of photosystem II. *Plant Cell Physiol* 42(2): 121–128.
16. Jansen MA, Mattoo AK, Edelman M (1999) D1-D2 protein degradation in the chloroplast. Complex light saturation kinetics. *Eur J Biochem* 260(2):527–532.
17. Frankel LK, Sallans L, Limbach PA, Bricker TM (2012) Identification of oxidized amino acid residues in the vicinity of the $Mn_{(4)}CaO_{(5)}$ cluster of Photosystem II: Implications for the identification of oxygen channels within the Photosystem. *Biochemistry* 51(32):6371–6377.
18. Sharma J, et al. (1997) Primary structure characterization of the photosystem II D1 and D2 subunits. *J Biol Chem* 272(52):33158–33166.
19. Frankel LK, Sallans L, Limbach PA, Bricker TM (2013) Oxidized amino acid residues in the vicinity of $Q_{(A)}$ and $Pheo_{(D1)}$ of the photosystem II reaction center: Putative generation sites of reducing-side reactive oxygen species. *PLoS One* 8(2):e58042.
20. Zavafer A, Cheah MH, Hillier W, Chow WS, Takahashi S (2015) Photodamage to the oxygen evolving complex of photosystem II by visible light. *Sci Rep* 5:16363.
21. Zhang H, et al. (2000) Detection of superoxide anion using an isotopically labeled nitrone spin trap: Potential biological applications. *FEBS Lett* 473(1):58–62.
22. Pou S, et al. (1994) A kinetic approach to the selection of a sensitive spin trapping system for the detection of hydroxyl radical. *Anal Biochem* 217(1):76–83.
23. Stadtman ER, Berlett BS (1991) Fenton chemistry. Amino acid oxidation. *J Biol Chem* 266(26):17201–17211.
24. Dean RT, Fu S, Stocker R, Davies MJ (1997) Biochemistry and pathology of radical-mediated protein oxidation. *Biochem J* 324(Pt 1):1–18.
25. Mason RP (2004) Using anti-5,5-dimethyl-1-pyrroline N-oxide (anti-DMPO) to detect protein radicals in time and space with immuno-spin trapping. *Free Radic Biol Med* 36(10):1214–1223.
26. Levine RL, et al. (1990) Determination of carbonyl content in oxidatively modified proteins. *Methods Enzymol* 186:464–478.
27. Miyao M, Ikeuchi M, Yamamoto N, Ono T (1995) Specific degradation of the D1 protein of photosystem II by treatment with hydrogen peroxide in darkness: Implications for the mechanism of degradation of the D1 protein under illumination. *Biochemistry* 34:10019–10026.
28. De Las Rivas J, Andersson B, Barber J (1992) Two sites of primary degradation of the D1-protein induced by acceptor or donor side photo-inhibition in photosystem II core complexes. *FEBS Lett* 301(3):246–252.
29. Mizusawa N, Yamamoto N, Murata N (1999) Characterization of damage to the D 1 protein of photosystem II under photoinhibitory illumination in non-phosphorylated and phosphorylated thylakoid membranes. *J Photochem Photobiol B* 48:97–103.
30. Lupínková L, Komenda J (2004) Oxidative modifications of the Photosystem II D1 protein by reactive oxygen species: From isolated protein to cyanobacterial cells. *Photochem Photobiol* 79(2):152–162.
31. Bricker TM, Mummadisetti MP, Frankel LK (2015) Recent advances in the use of mass spectrometry to examine structure/function relationships in photosystem II. *J Photochem Photobiol B* 152(Pt B):227–246.
32. Frankel LK, et al. (2013) Radiolytic mapping of solvent-contact surfaces in Photosystem II of higher plants: Experimental identification of putative water channels within the photosystem. *J Biol Chem* 288(32):23565–23572.
33. Arató A, Bondarava N, Krieger-Liszkay A (2004) Production of reactive oxygen species in chloride- and calcium-depleted photosystem II and their involvement in photoinhibition. *Biochim Biophys Acta* 1608(2-3):171–180.
34. Semin BK, et al. (2013) Production of reactive oxygen species in decoupled, $Ca^{(2+)}$-depleted PSII and their use in assigning a function to chloride on both sides of PSII. *Photosynth Res* 117(1-3):385–399.
35. Yadav DK, Pospíšil P (2012) Role of chloride ion in hydroxyl radical production in photosystem II under heat stress: Electron paramagnetic resonance spin-trapping study. *J Bioenerg Biomembr* 44(3):365–372.
36. Mavankal G, McCain DC, Bricker TM (1986) Effects of chloride on paramagnetic coupling of manganese in calcium chloride-washed Photosystem II preparations. *FEBS Lett* 202:235–239.
37. Kawakami K, Umena Y, Kamiya N, Shen J-R (2009) Location of chloride and its possible functions in oxygen-evolving photosystem II revealed by X-ray crystallography. *Proc Natl Acad Sci USA* 106(21):8567–8572.
38. Wincencjusz H, van Gorkom HJ, Yocum CF (1997) The photosynthetic oxygen evolving complex requires chloride for its redox state S2—>S3 and S3—>S0 transitions but not for S0—>S1 or S1—>S2 transitions. *Biochemistry* 36(12):3663–3670.
39. Wincencjusz H, Yocum CF, van Gorkom HJ (1999) Activating anions that replace Cl- in the O2-evolving complex of photosystem II slow the kinetics of the terminal step in water oxidation and destabilize the S2 and S3 states. *Biochemistry* 38(12):3719–3725.
40. Najafpour MM, et al. (2016) Manganese compounds as water-oxidizing catalysts: From the natural water-oxidizing complex to nanosized manganese oxide Ssructures. *Chem Rev* 116(5):2886–2936.
41. Berthold DA, Babcock GT, Yocum CF (1981) A highly resolved oxygen-evolving Photosystem II preparation from spinach thylakoid membranes. *FEBS Lett* 134:231–234.
42. Ford RC, Evans MCW (1983) Isolation of a Photosystem 2 preparation from higher plants with highly enriched oxygen evolution activity. *FEBS Lett* 160:159–164.
43. Ghanotakis DF, Babcock GT (1983) Hydroxylamine as an inhibitor between Z and P_{680} in Photosystem II. *FEBS Lett* 153:231–234.
44. Schägger H (2006) Tricine-SDS-PAGE. *Nat Protoc* 1(1):16–22.
45. Rabilloud T, Vincon M, Garin J (1995) Micropreparative one- and two-dimensional electrophoresis: Improvement with new photopolymerization systems. *Electrophoresis* 16(8):1414–1422.
46. Sun G, Anderson VE (2004) Prevention of artifactual protein oxidation generated during sodium dodecyl sulfate-gel electrophoresis. *Electrophoresis* 25(7-8):959–965.
47. Xu H, Freitas MA (2007) A mass accuracy sensitive probability based scoring algorithm for database searching of tandem mass spectrometry data. *BMC Bioinformatics* 8:133–137.
48. Xu H, Freitas MA (2009) MassMatrix: A database search program for rapid characterization of proteins and peptides from tandem mass spectrometry data. *Proteomics* 9(6):1548–1555.
49. Xu G, Chance MR (2005) Radiolytic modification and reactivity of amino acid residues serving as structural probes for protein footprinting. *Anal Chem* 77(14):4549–4555.
50. Kiselar JG, Chance MR (2010) Future directions of structural mass spectrometry using hydroxyl radical footprinting. *J Mass Spectrom* 45(12):1373–1382.
51. DeLano WL (2002) *The PyMOL Molecular Graphics System* (Schrödinger, New York).